SLAC-PUB-5004
August 1989
(E)

MULTIPLE-NEUTRAL-MESON DECAYS OF THE τ LEPTON AND ELECTROMAGNETIC CALORIMETER REQUIREMENTS AT TAU–CHARM FACTORY*

K. K. GAN
Stanford Linear Accelerator Center
Stanford University, Stanford, CA 94309

ABSTRACT

This is a study of the physics sensitivity to the multiple-neutral-meson decays of the τ lepton at the Tau-Charm Factory. The sensitivity is compared for a moderate and an ultimate electromagnetic calorimeter. With the high luminosity of the Tau-Charm Factory, a very large sample of the decays $\tau^- \to \pi^- 2\pi^0 \nu_\tau$ and $\tau^- \to \pi^- 3\pi^0 \nu_\tau$ can be collected with both detectors. However, with the ultimate detector, $2\pi^0$ and $3\pi^0$ can be unambiguously reconstructed with very little background. For the suppressed decay $\tau^- \to \pi^- \eta\pi^0 \nu_\tau$, only the ultimate detector has the sensitivity. The ultimate detector is also sensitive to the more suppressed decay $\tau^- \to K^- \eta \nu_\tau$ and the moderate detector may have the sensitivity if the hadronic background is not significantly larger than that predicted by Lund. In the case of the highly suppressed second-class-current decay $\tau^- \to \pi^- \eta \nu_\tau$, only the ultimate detector has sensitivity. The sensitivity can be greatly enhanced with a small-angle photon veto.

1. INTRODUCTION

The discrepancy[1] between the inclusive and the sum of the exclusive one-charged-particle decay branching ratios of the τ lepton remains a perplexing problem[2] in the Standard Model. Solving the discrepancy is one of the foremost missions of the Tau-Charm Factory. The decays with multiple-neutral mesons in the final states are the least understood and the electromagnetic calorimeter will be crucial in unravelling the paradox. The calorimeter is of particular importance in view of the apparent excess[3] of the multiple-

Invited talk presented at the Tau-Charm Factory Workshop, Stanford, CA, May 23–27, 1989.

* Work supported by Department of Energy contract DE–AC03–76SF00515.

neutral-meson decay modes over the theoretical expectations. Even if the paradox is solved by the time the Tau-Charm Factory is built, the high luminosity still allows high-precision tests of the Standard Model in these modes and the observation of the highly suppressed decays, such as $\tau^- \to K^-\eta\nu_\tau$ and the second-class-current decay $\tau^- \to \pi^-\eta\nu_\tau$. The electromagnetic calorimeters assumed in these studies are discussed in Sec. 2. The sensitivity to various decay modes are discussed in Sec. 3. The results are summarized in Sec. 4.

2. ELECTROMAGNETIC CALORIMETER

Two kinds of electromagnetic calorimeters are compared in the study: a moderate calorimeter, like an upgraded Mark III detector, and an ultimate detector, similar to the CsI(Tl) detector of CLEO II. Both detectors consist of a barrel and two endcaps, with the barrel located at R = 1.1 m and the endcaps at $Z = \pm 1.9$ m. The endcaps extend in polar angle down to $|\cos\theta| = 0.95$. Both the barrel and endcaps have an azimuthal angular resolution of $\Delta\phi$ = 10 mrad. The barrel has a longitudinal resolution of AZ = ± 2 cm and the endcaps have a radial resolution of AR = ± 2 cm. The two-photon separation resolution is 4 cm. For the moderate detector, there is a crack between the barrel and endcaps of $|\Delta \cos\theta| = 0.01$. No crack is assumed for the ultimate detector.

The energy resolution of the moderate detector is assumed to be

$$\sigma/E = 8\%/\sqrt{E} + 1\% \quad ,$$

where the electromagnetic energy E is expressed in units of GeV. A moderate photon-detection efficiency is assumed as shown in Fig. 1. For the ultimate detector, the energy resolution is

$$\sigma/E = 2\%/\sqrt{E} + 1\% \, ,$$

and a very high photon detection efficiency down to very low energy is assumed (see Fig. 1). This type of detection efficiency will match well with the energy spectrum of the photons from τ decay (Fig. 2) and minimize the migration of high photon multiplicity events to lower multiplicity. To achieve this type of efficiency, a nonsampling detector is required. A crystal detector like CsI(Tl) is a natural candidate. The detection efficiency for low-energy

photons is limited by noise and absorption by the material in front of the crystal. In this study, an efficiency of 90% is assumed for photons with energy between 10 and 20 MeV. Noise will not be a limiting factor because a noise level below 1 MeV is achievable.[4] The bulk of material in front of the calorimeter will come from the drift chamber aluminum outer wall and end plates, as the beam pipe and the inner drift chamber wall can be made of beryllium. Using the new Mark II drift chamber as an example, the probability of interaction for a 10 MeV photon is shown in Table I. Averaged over the 4π solid angle, the probability is $\sim$ 8%. The 90% detection efficiency assumed for a 10–20 MeV photon is therefore attainable. In fact, this is a conservative estimate because we have assumed that the photon is totally absorbed. In reality, some energy will be detected by the calorimeter and for a photon with energy close to 20 MeV, there will be enough energy deposited in the calorimeter to pass the 10 MeV threshold used in this study. To enhance the probability of detecting the interacting photon as a single photon, the distance between the barrel and endcap calorimeter and the drift chamber outer wall and end plates should be minimal. This prevents the shower of the interacting photon from spreading over many crystals and creating spurious photons. In the efficiency calculation, we assume that the energy deposited in the time-of-flight system (TOF) can be added to the calorimeter. Since the π^0's from the τ decay will be emitted almost isotropically because the τ is produced near threshold, some photons will escape detection through the holes around the beam pipe. It is therefore important to instrument these holes with electromagnetic shower detector, e.g., BGO. The current machine design allows for instrumentation down to $|\cos\theta| = 0.99$ and possibly down to 0.995. It is also important to keep the shower energy threshold as low as possible. The background in the highly suppressed decays will be studied with various veto scenarios: no veto, and veto with threshold energies of 50 and 100 MeV and angular coverage of $|\cos\theta| = 0.95$ to 0.99 and 0.95 to 0.995.

3. PHYSICS SENSITIVITY

The physics sensitivity to various decay modes is studied at $\sqrt{s}$ = 3.67 GeV using a Monte Carlo technique. In the Monte Carlo, the τ decays with the known branching ratios.[7] The energy and momentum of the decay products are then smeared with the resolution expected for a Tau-Charm Factory detector, using a program written by R. Schindler and

coworkers for this workshop. In the analysis, a τ sample of 40 $\times$ 10^6 events is assumed. The hadronic background is calculated using Lund[6] (Version 6.2). The Monte Carlo does not reproduce the data at this energy very well. Therefore, the prediction is only reliable[7] to within a factor of 2.

A. $\tau^- \rightarrow \pi^- 2\pi^0\nu_\tau$

The decay $\tau^- \rightarrow \pi^- 2\pi^0\nu_\tau$ is the second largest decay mode with π^0's in the final state. Due to the multiple photons in the decay, reconstruction of this mode required goodenergy resolution and detection efficiency to minimize feeddown from higher photon multiplicity states. There is only one direct measurement of the branching ratio (Crystal Ball Collaboration),[8] but there are several indirect measurements through photon counting and/or partial π^0 reconstruction. The weighted average of these measurements[5] is

$$B(\tau^- \rightarrow \pi^- 2\pi^0\nu_\tau) = (7.5 \pm 0.7)\% ,$$

assuming there is no correlation in systematic errors between different experiments. The branching ratio is related to the three-charged-gion decay by isospin invariance,

$$B(\tau^- \rightarrow \pi^- 2\pi^0\nu_\tau) \leq B(\tau^- \rightarrow \pi^- \pi^+ \pi^-\nu_\tau) .$$

In principle, the three-charged-particle branching ratio is much easier to measure. However, there is significant discrepancy between different experiments. It is therefore important to measure $B(\tau^- \rightarrow \pi^- 2\pi^0\nu_\tau)$ directly with good precision. The measurement will also elucidate the apparent excess in the multiple-neutral-meson branching ratios over the theoretical expectations. Note that the three-charged-particle branching ratio can be measured precisely in the same experiment, allowing an accurate test of isospin invariance, since many systematic errors will cancel.

The event selection criteria are quite simple and designed primarily to reject the hadronic background. The event is required to contain two charged tracks and four photons. At least one of the tracks must be an electron or muon. An electron candidate is defined as a particle that deposits a shower energy that is within 20% of the expected value calculated from the track momentum for the moderate detector and within 10% for the

ultimate detector. A muon candidate is identified through a look-up table which represents the realistic identification efficiency as a function of momentum, achievable using a combination of dE/dx, TOF and penetrating power. Pion misidentification is also included through a look-up table. Each photon is required to have a minimum energy of 10 MeV. The total neutral energy in the hadronic calorimeter must be less than 50 MeV and the total visible energy, excluding the hadronic calorimeter energy, must be less than 2.3 GeV. The hadronic background can be further suppressed by using the fact that the τ candidate should contain no kaon other than misidentification, but a fair fraction of the hadronic events contain kaons. The kaons in the hadronic events are produced either directly in $e^+e^- \rightarrow s\bar{s}$ or through $s\bar{s}$ popping from the sea. Therefore, any event that contains a kaon candidate identified through the TOF information is rejected. No dE/dx information is used; including this information will further suppress the background. However, the kaon momentum is soft and may decay inside the detector, causing the expected TOF to be miscalculated. Fortunately, the kink in the track may cause the vertex to be poorly measured; therefore, any event with distance of closest approach in the xy plane greater than 5 mm is rejected.

The expected number of events passing the selection criteria are summarized in Table II, together with the background. For both types of detectors, there are about one million events and therefore, the measurement will be limited by systematics. The inclusive $\gamma\gamma$ mass spectra are shown in Figs. 3(a) and 4(a). A clean π^0 signal is evident. To demonstrate that the four-photon events are dominated by $\tau^- \rightarrow \pi^- 2\pi^0\nu_\tau$, Figs. 3(b) and 4(b) show the mass spectrum of the $\gamma\gamma$ pair recoiling against a π^0 candidate, with the π^0 resolution taken to be 50 $\mathrm{MeV/c^2}$ for the moderate detector and 20 $\mathrm{MeV/c^2}$ for the ultimate detector. The background under the π^0 peak is small for the moderate detector and negligible for the ultimate detector. The hadronic background is small and not included in the mass spectrum. The contamination is more than a factor of 2 smaller with the ultimate detector. Note that we have a photon energy threshold of 10 MeV for both detectors. This may not be realistic for the moderate detector. A higher threshold could greatly reduce the detection efficiency and increase the contamination from $\tau^- \rightarrow \pi^- 3\pi^0\nu_\tau$ and hadrons, and hence have a much larger systematic error. In summary, both detectors are adequate for studying the decay $\tau^- \rightarrow \pi^- 2\pi^0\nu_\tau$, and the ultimate detector will have a much smaller systematic error.

B. $\tau^- \to \pi^- \eta \pi^0 \nu_\tau$

The branching ratio for $\tau^- \to \pi^- \eta \pi^0 \nu_\tau$ can be calculated from the cross section for $e^+e^- \to \eta \pi^+\pi^-$ using the Conserved-Vector-Current (CVC) Hypothesis.[9] The prediction" is

$$B(\tau^- \to \pi^- \eta \pi^0 \nu_\tau) = (0.13 \pm 0.02)\% .$$

Because of this small branching ratio and the large combinatorial background from $\tau^- \to \pi^- 2\pi^0 \nu_\tau$, the decay is yet to be observed.

The selection criteria are identical to those for $\tau^- \to \pi^- 2\pi^0 \nu_\tau$. This is no hint of a signal in the inclusive $\gamma\gamma$ mass spectra shown in Figs. 3(a) and 4(a). However, when the $\gamma\gamma$ pair is required to recoil against a π^0 candidate, a signal is observed with the ultimate detector [Fig. 4(c)] but not with the moderate detector [Fig. 3(c)]. The spectra correspond to $\sim 1/150$ of the final data sample.[11] We can expect $\sim$ 7500 candidate events for $\tau^- \to \pi^- \eta \pi^0 \nu_\tau$ in the final sample. The error in the branching ratio will be much smaller than the uncertainty in the theoretical prediction, which is dominated by the statistical uncertainty in the e^+e^- cross section. It is important to measure the cross section to higher precision; the Tau-Charm Factory will be an excellent facility for such measurement.[12]

C. $\tau^- \to \pi^- 3\pi^0 \nu_\tau$

The decay $\tau^- \to \pi^- 3\pi^0 \nu_\tau$ is related to the process $e^+e^- \to \pi^+\pi^-\pi^+\pi^-$ by CVC. Since the e^+e^- process has no photon in the final state, the cross section can be measured with good precision and the decay branching ratio is predicted[13] to be

$$B(\tau^- \to \pi^- 3\pi^0 \nu_\tau) = 1.0\% .$$

However, with the multiple photons in the τ decay, it is difficult to measure the branching ratio and there is essentially no direct measurement.'

The selection criteria are identical to those for $\tau^- \to \pi^- 2\pi^0 \nu_\tau$, except for the photon multiplicity requirement. The number of events passing the selection criteria for the two detectors is summarized in Table II, together with the hadronic background. In both detectors, we expect $\sim 10^5$ events and the branching ratio measurement will be limited

by systematics. The inclusive $\gamma\gamma$ mass spectra are shown in Figs. 5(a) and 6(a). There is an indication of a π^0 signal for the moderate detector and a clear π^0 signal for the ultimate detector on top of the large combinatorial background. When the $\gamma\gamma$ pair is required to recoil against two π^0 candidates for the moderate detector, the combinatorial background is substantially reduced, but remains large. To measure the branching ratio with high precision will require a good understanding of the shape of the background. For the ultimate detector, the background is negligible and flat, allowing the branching ratio to be measured with small systematic error. The hadronic contamination for the moderate detector is at $\sim$ 13% level, and for the ultimate detector is about a factor of 2 smaller. In summary, both detectors will yield a large sample of 6γ events. However, only the ultimate detector can ambiguously reconstruct the $3\pi^0$ with negligible background and hence allows a precise measurement of the branching ratio to test CVC.

D. $\tau^- \rightarrow K^- \eta\nu_\tau$

The decay $\tau^- \rightarrow K^- \eta\nu_\tau$ is allowed in the Standard Model but suppressed. The branching ratio has been estimated using a Chiral Effective Lagrangian by A. Pich,[14]

$$B(\tau^- \rightarrow K^- \eta\nu_\tau) \simeq 1.2 \times 10^{-4} .$$

The decay has, of course, not yet been observed.

The selection criteria are identical to those for $\tau^- \rightarrow \pi^- 2\pi^0\nu_\tau$, except for three changes. First, there must be at least one kaon in the event, identified using the TOF information. Second, the total neutral electromagnetic energy must be between 0.5 and 1.1 GeV. Third, there must be exactly two photons with energy greater than 100 MeV and no other photon above 10 MeV. The second and third requirements are imposed using the fact that, with the relatively small number of particles in the final state, the energy spectrum of the η is quite narrow and the photons from the η decay are quite energetic.

The invariant mass spectra of the two photons for the two types of calorimeter are shown in Fig. 7. The hadronic background is large and also peaks at the η mass. This is due to the fact that the event is tagged with a kaon and an η is likely to be produced with the kaon because of the $s\bar{s}$ content of the η. This large background must be calculated precisely in order to measure the branching ratio; a calculation that can only be done by measuring

the background below the τ threshold. Assuming that the background can be calculated precisely, a signal for $\tau^- \to K^- \eta\nu_\tau$ can be established with the ultimate detector and also may be established with the moderate detector if the hadronic background actually measured from the data is not significantly larger than that predicted by Lund. A signal of $\sim$ 500 events is expected for the moderate detector and $\sim$ 600 events for the ultimate detector. The background can be further suppressed by a small angle veto. If photons with energy above 100 MeV in the angular range $|\cos\theta|$ = 0.95 to 0.99 are vetoed, the background can be reduced by about a factor of 2 with negligible loss of signal.

E. $\tau^- \to \pi^- \eta\nu_\tau$

The decay $\tau^- \to \pi^- \eta\nu_\tau$ is of particular interest in the Standard Model of electroweak interaction. The G-parity of the $\pi\eta$ system is opposite to that for a first-class current. The decay is strongly suppressed in the Standard Model. In the isospin limit with equal masses for the light quarks, second-class currents vanish altogether. Isospin violations are naturally expected to be of order α^2, so a branching ratio suppressed by order 10^{-5} is expected. Observation of a sizable branching ratio could indicate the existence of second-class currents. Of course, it also could indicate G-parity violation in the strong interaction hadronization process after the virtual W decays into quarks, or other nonstandard decay mechanisms, such as the existence of a new scalar particle (Higgs). The simplicity of the decay process, $\tau^- \to \pi^- \eta\nu_\tau \to \pi^-\gamma\gamma\nu_\tau$, provides a clean laboratory for the search[15] for second-class currents. This is in sharp contrast to the searches[16] in nuclear β decay and muon capture, which are at small momentum transfer and complicated by nuclear form factors. The branching ratio is predicted to be[14]

$$B(\tau^- \to \pi^- \eta\nu_\tau) \simeq 1.5 \times 10^{-5} ,$$

and is expected to proceed through the $a_0(980)$ resonance. Observation of the decay should be a major goal of the Tau-Charm Factory.

The selection criteria are identical to those for $\tau^- \to K^-\eta\nu_\tau$, except for two changes. First, no kaon is allowed. Second, when the two photons are combined with one of the charged particles, there must be at least one combination that is consistent with the a_0 hypothesis. The a_0 resolution is taken to 100 MeV/c^2 for the moderate detector and

70 MeV/c^2 for the ultimate detector. The $\gamma\gamma$ mass spectra for the two detectors are shown in Fig. 8. The moderate detector has no sensitivity to the η signal due to the large feeddown from the higher photon multiplicity decays resulting from the limited detection efficiency for low-energy photons. For the ultimate detector, an η signal corresponding to $\sim$ 100 events is observed. The hadronic background is not included in the mass spectra, but is small for the ultimate detector.

The η signal observed with the ultimate detector can be greatly enhanced with a small--angle photon veto. Three veto scenarios are considered:

(a) a veto with 100 MeV threshold in the angular region $|\cos\theta|$ = 0.95 to 0.99;

(b) same as (a), but with 50 MeV threshold;

(c) 50 MeV threshold for $|\cos\theta|$ = 0.95 to 0.995.

The mass spectra with these vetoes are shown in Fig. 9. The background is strongly suppressed with negligible loss of signal.

In summary, the Tau-Charm Factory is sensitive to second-class currents only with the ultimate detector and the sensitivity can be greatly enhanced with a small-angle photon veto.

4. CONCLUSIONS

The study of the multiple-neutral-meson decays of the τ is a struggle with the current detectors at the existing e^+e^- colliders. With the high luminosity of the Tau-Charm Factory, the decays can be systematically studied. We can expect a very large sample of four- and six-photon $(10^5$–$10^6)$ events. With the ultimate detector, $2\pi^0$ and $3\pi^0$ can be unambiguously reconstructed. Also, only the ultimate detector has the sensitivity to the suppressed decay $\tau^- \rightarrow \pi^-\eta\pi^0\nu_\tau$. The ultimate detector is also sensitive to the more suppressed decay $\tau^- \rightarrow K^-\eta\nu_\tau$ and the moderate detector may have the sensitivity if the hadronic background is not significantly larger than that predicted by Lund. For the highly suppressed second-class-current decay $\tau^- \rightarrow \pi^-\eta\nu_\tau$, only the ultimate detector has the sensitivity. The sensitivity can be greatly enhanced with a small-angle photon veto. In all the decays, the combinatorial, migration, and hadronic backgrounds are much smaller

with the ultimate detector, thus reducing a potential source of systematic error. If the τ – paradox persists during the Tau-Charm Factory era, the paradox can be unravelled with the excellent energy resolution and detection efficiency provided by the ultimate detector. In conclusion, a detector with the capacity of the ultimate detector is highly recommended.

The author wishes to thank G. Grindhammer and C. Munger for useful discussions. This work has been made possible by the Monte Carlo program of R. Schindler and coworkers.

REFERENCES

1. F. J. Gilman and S. H. Rhie, Phys. Rev. **D31**, 1066 (1988).
2. For recent reviews, ***see*** K. K. Gan, ***Proceedings of the 23rd Rencontre de Moriond: 88 Electroweak Interactions. and Unified Theories,*** Les Arcs, Sovoie, France (1988), ed. J. Tran Thanh Van, p. 399;
   C. Kiesling, to be published in ***Proceedings of the 24th Rencontre de Moriond,*** Les Arcs, Sovoie, France (1989).
3. K. K. Gan ***et al.,*** Phys. Rev. Lett. 59, 411 (1987);
   H. Aihara ***et al.,*** Phys. Rev. Lett. 57, 1836 (1986);
   H. R. Band ***et al.,*** Phys. Lett. **198B**, 297 (1987).
4. E. Blucher ***et al.,*** Nucl. Instr. and Meth. **A249**, 201 (1986).
5. K. K. Gan of Ref. 2.
6. T. Sjöstrand, Comp. Phys. Comm. 39, 347 (1986).
7. Private communication, G. Grindhammer.
8. ***S.*** T. Lowe, ***Proceedings of the International Symposium of Production and Decay of Heavy Flavors*** (Stanford, CA, 1987), ed. E. Bloom and A. Fridman, p. 527.
9. R. P. Feynman and M. Gell-Mann, Phys. Rev. 109, 193 (1958).
10. A. Antonelli ***et*** al., Phys. Lett. **212B**, 133 (1988).
11. Figures 3-6 correspond to $\sim 1/150$ of the full data sample, and all following figures correspond to the full data sample.
12. K. K. Gan, these proceedings.
13. Y. S. Tsai, Phys. Rev. D4, 2821 (1971) and Ref. 1.
14. A. Pich, Phys. Lett. **196B**, 561 (1987).
15. C. Leroy and J. Pestieau, Phys. Lett. **72B**, 398 (1978);
    S. N. Biswas ***et*** al., Phys. Lett. SOB, 393 (1979);
    N. Paver and D. Treleani, Lett. Nuovo Cimento 31, 364 (1981);
    V. P. Barannik, A. P. Korzh and M. P. Rekalo, Acta Phys. Pol. **B13**, 835 (1982).
16. L. Grenacs, Ann. Rev. Nucl. Part. Sci. 35, 455 (1985).

TABLES

Table I. Probability of interaction for a 10 MeV photon in the material in front of the electromagnetic calorimeter.

Material	Thickness (mm)	Probability (%)
Beam pipe (Be)	0.5	0.2
Inner DC wall (Be)	2.0	0.7
Outer DC wall (Al)	12.7	6.6
DC end plate (Al)	51.0	24.1

Table II. The expected number of signal and hadronic background events for $\tau^- \to \pi^- 2\pi^0\nu_\tau$ and $\tau^- \to \pi^- 3\pi^0\nu_\tau$ detected with the moderate and ultimate calorimeters.

Topology	Calorimeter	Events	Background (%)
$\tau^- \to \pi^- 2\pi^0\nu_\tau$	moderate	1.1 x 10^6	5.6
	ultimate	1.7 x 10^6	2.1
$\tau^- \to \pi^- 3\pi^0\nu_\tau$	moderate	1.3 x 10^5	12.9
	ultimate	2.3 x 10^5	7.3

FIGURE CAPTIONS

1. Photon detection efficiency assumed in the study for a moderate (dashed) and an ultimate (full) detectors.

2. The raw energy spectrum of the photons from τ decay (arbitrary normalization).

3. The $\gamma\gamma$ mass spectrum of four-photon candidate events for $\tau^- \to \pi^- 2\pi^0 \nu_\tau$ detected with a moderate calorimeter: (a) all $\gamma\gamma$ pairs; (b) $\gamma\gamma$ pairs that recoiled against a π^0 candidate; (c) enlarged view of (b).

4. The $\gamma\gamma$ mass spectrum of four-photon candidate events for $\tau^- \to \pi^- 2\pi^0 \nu_\tau$ detected with an ultimate calorimeter: (a) all $\gamma\gamma$ pairs; (b) $\gamma\gamma$ pairs that recoiled against a π^0 candidate; (c) enlarged view of (b).

5. The $\gamma\gamma$ mass spectrum of six-photon candidate events for $\tau^- \to \pi^- 3\pi^0 \nu_\tau$ detected with a moderate calorimeter: (a) all $\gamma\gamma$ pairs; (b) $\gamma\gamma$ pairs that recoiled against two π^0 candidates.

6. The $\gamma\gamma$ mass spectrum-of six-photon candidate events for $\tau^- \to \pi^- 3\pi^0 \nu_\tau$ detected with an ultimate calorimeter: (a) all $\gamma\gamma$ p-airs; (b) $\gamma\gamma$ pairs that recoiled against two π^0 candidates.

7. The $\gamma\gamma$ mass spectrum of the candidate events for $\tau^- \to K^- \eta \nu_\tau$: (a) the moderate detector; (b) the ultimate detector.

8. The $\gamma\gamma$ mass spectrum of the candidate events for $\tau^- \to \pi^- \eta \nu_\tau$: (a) the moderate detector; (b) the ultimate detector.

9. The $\gamma\gamma$ mass spectrum of the candidate events for $\tau^- \to \pi^- \eta \nu_\tau$ detected with the ultimate calorimeter for various small-angle photon veto scenarios (see text).

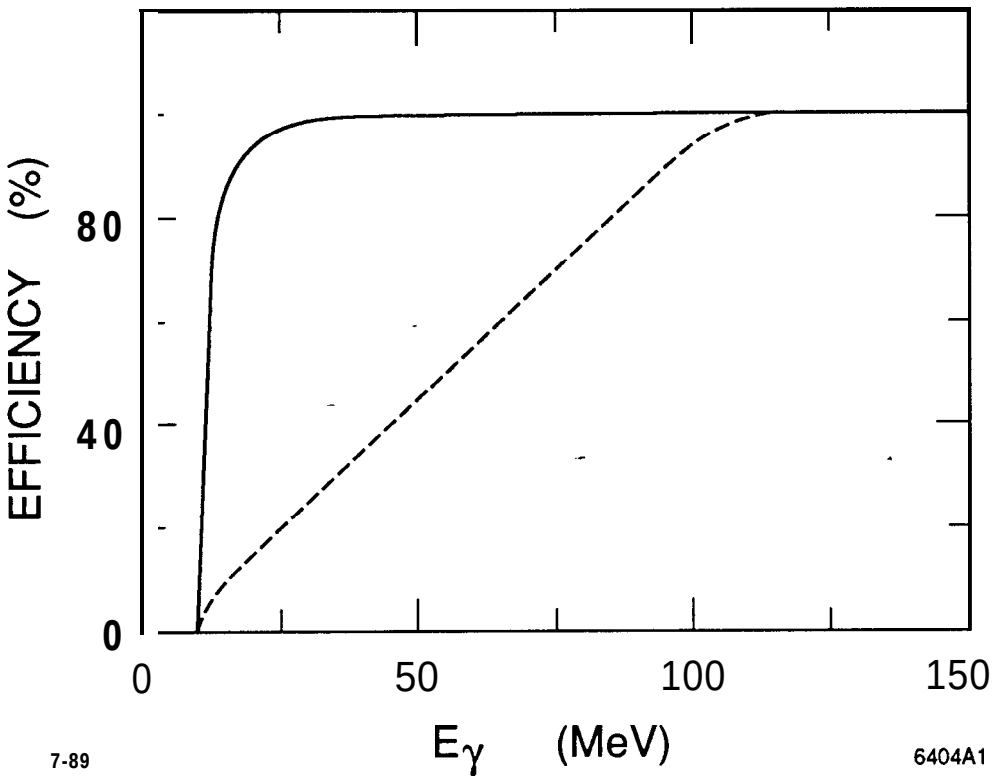

Fig. 1

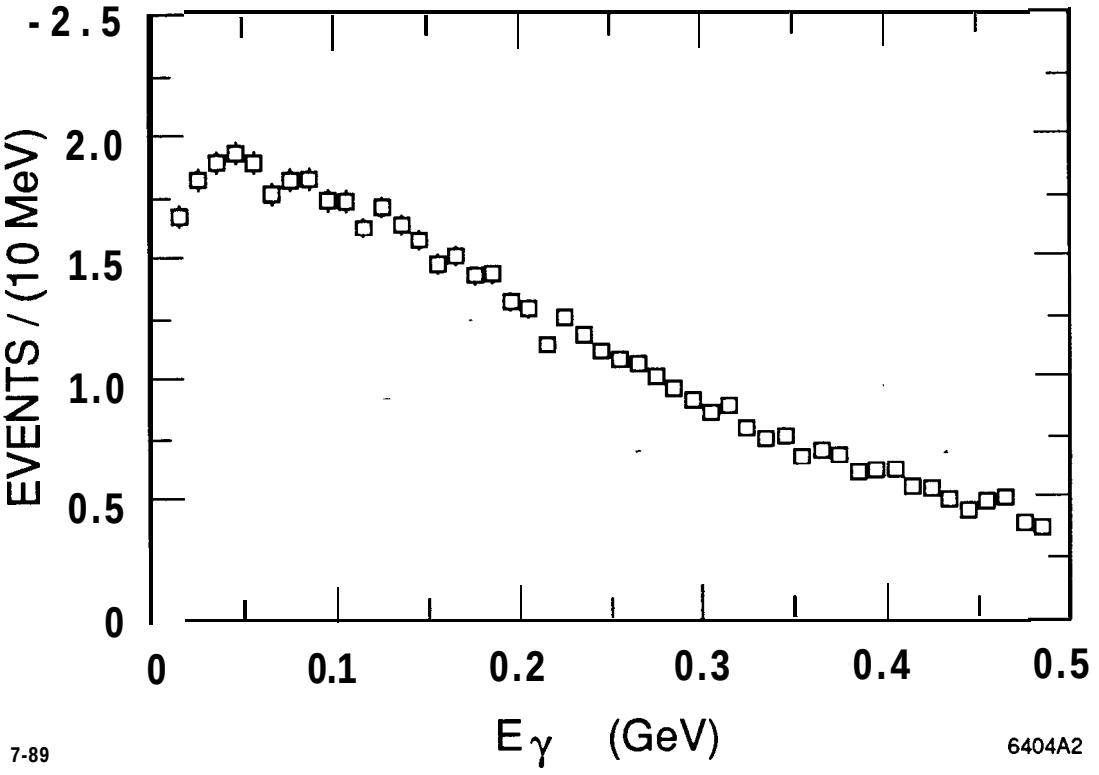

Fig. 2

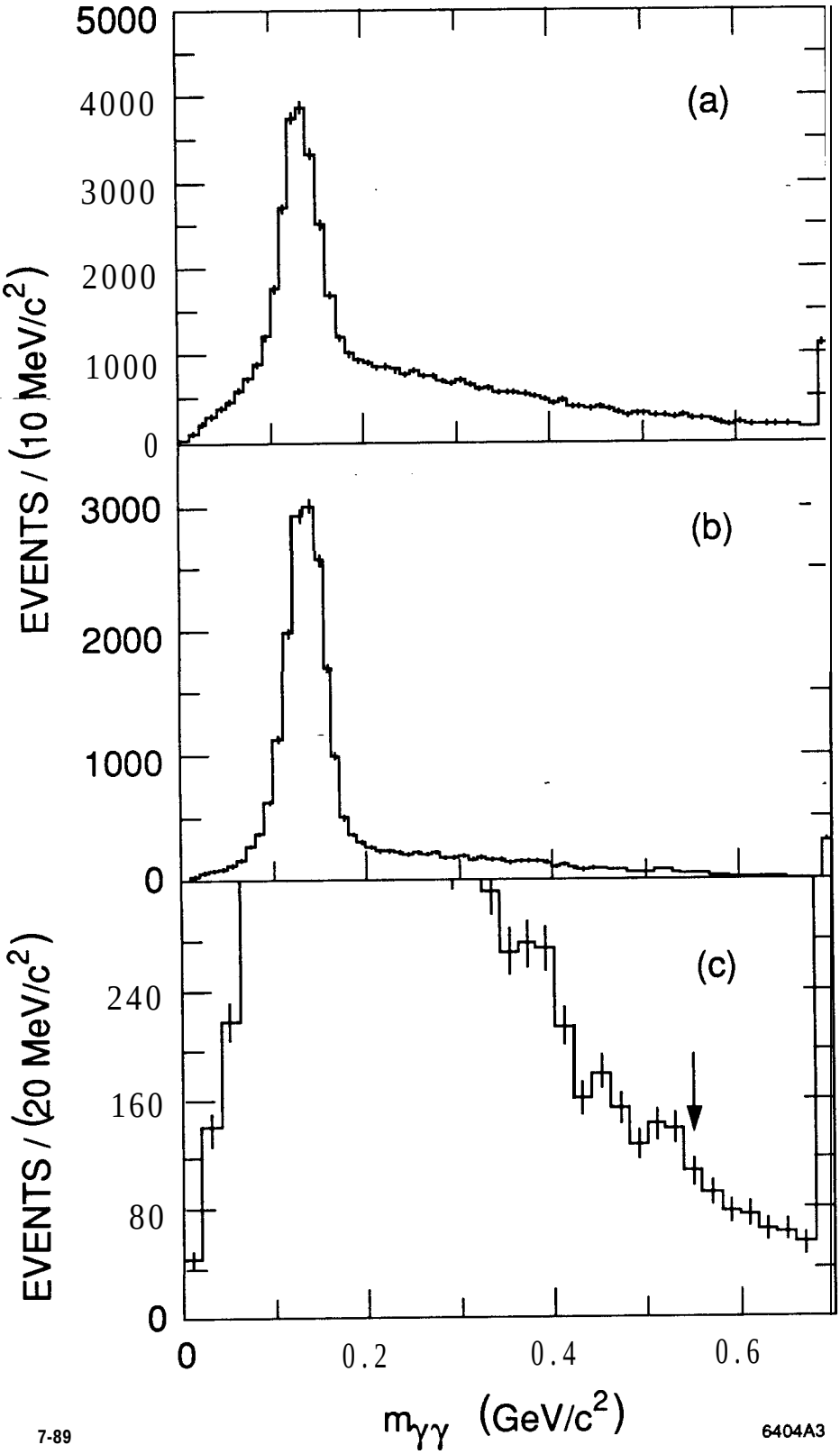
5000
4000
3000
2000
1000
0
(a)
EVENTS / (10 MeV/c²)
3000
2000
1000
0
(b)
240
160
80
0
(c)
EVENTS / (20 MeV/c²)
0
0.2
0.4
0.6
mγγ (GeV/c²)
7-89
6404A3

Fig. 3

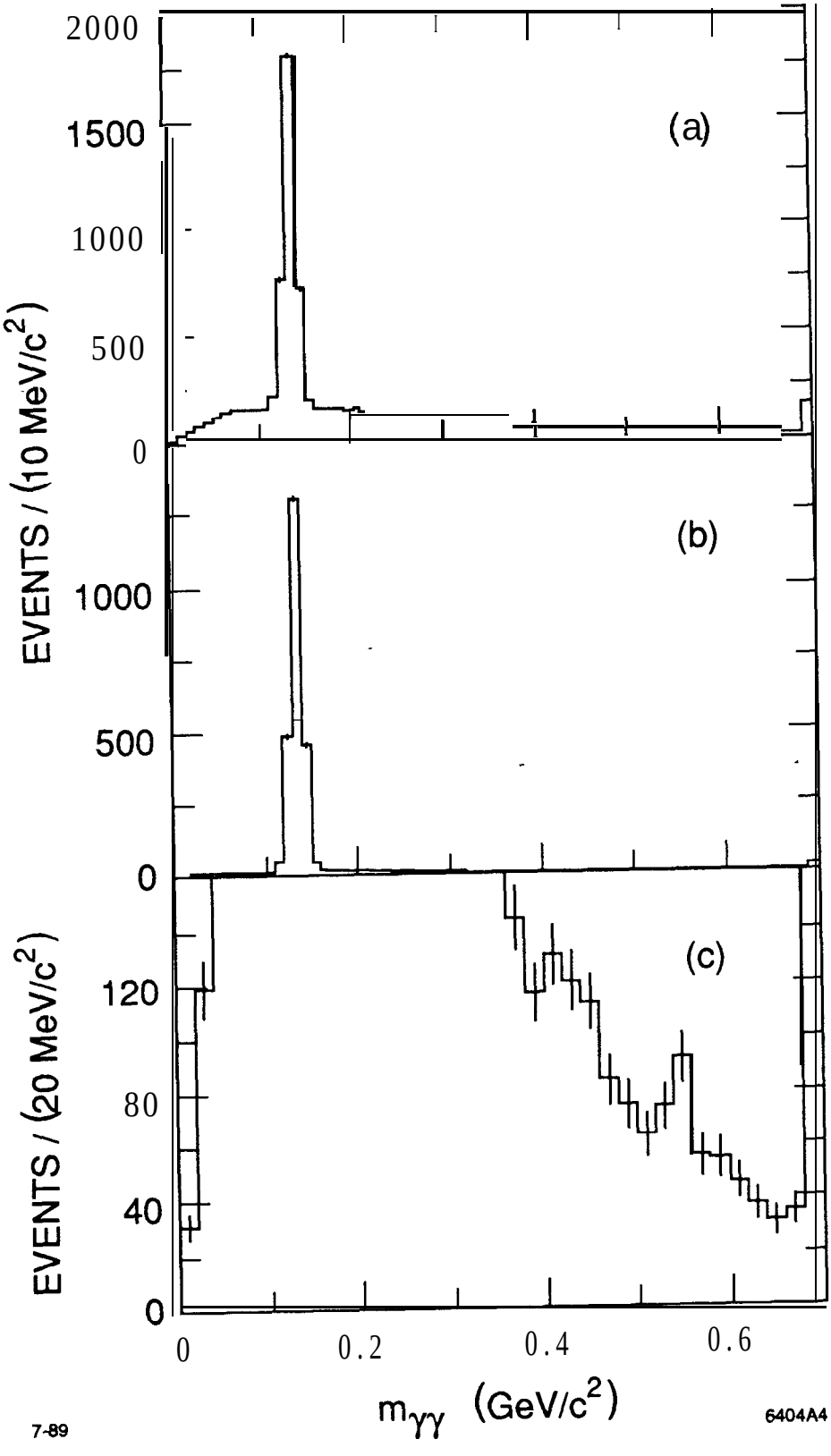
2000
1500
1000
500
0
(a)
EVENTS / (10 MeV/c²)
1000
500
0
(b)
EVENTS / (20 MeV/c²)
120
80
40
0
(c)
0
0.2
0.4
0.6
mγγ (GeV/c²)
7-89
6404A4

Fig. 4

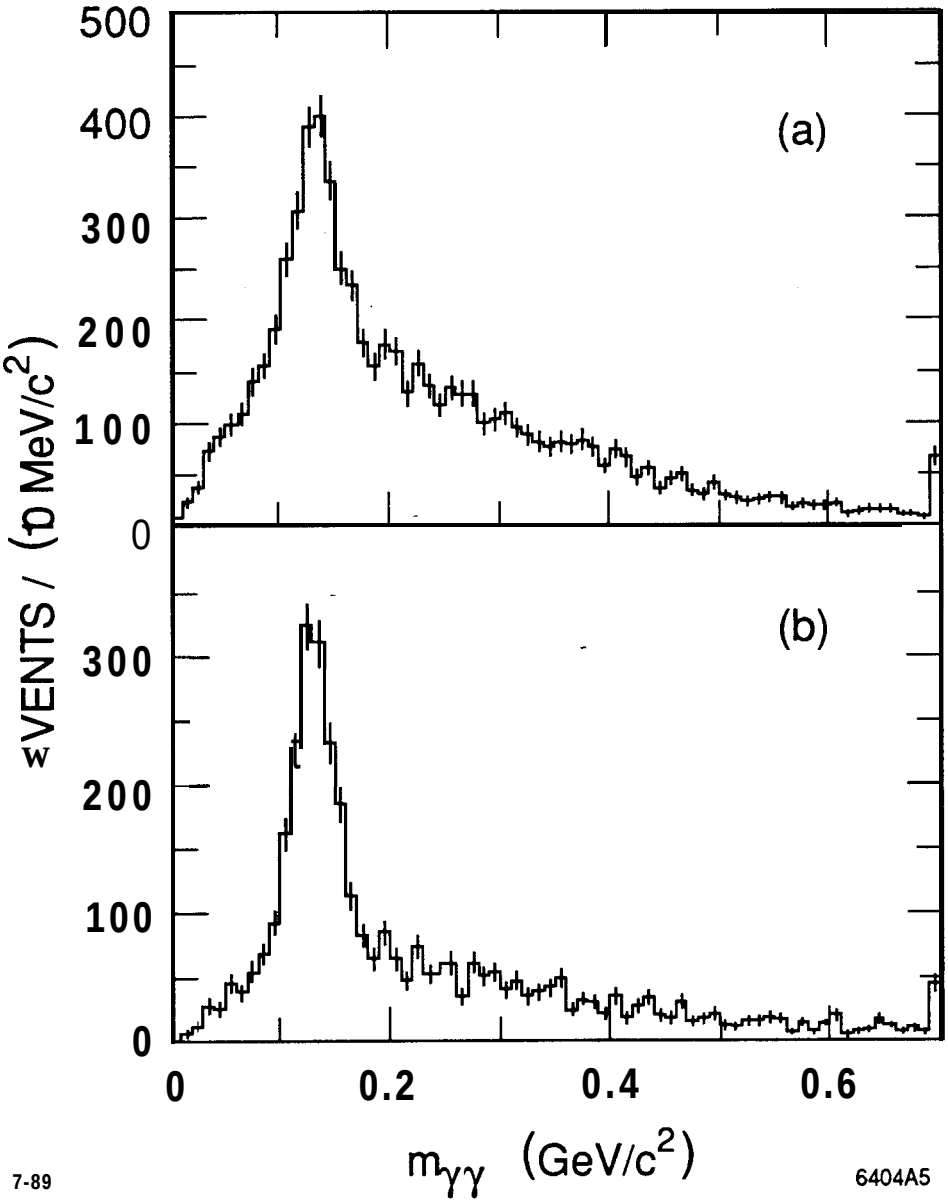
500
400
300
200
100
0
(a)
(b)
300
200
100
0
0
0.2
0.4
0.6
EVENTS / (10 MeV/c²)
mγγ (GeV/c²)
7-89
6404A5

Fig. 5

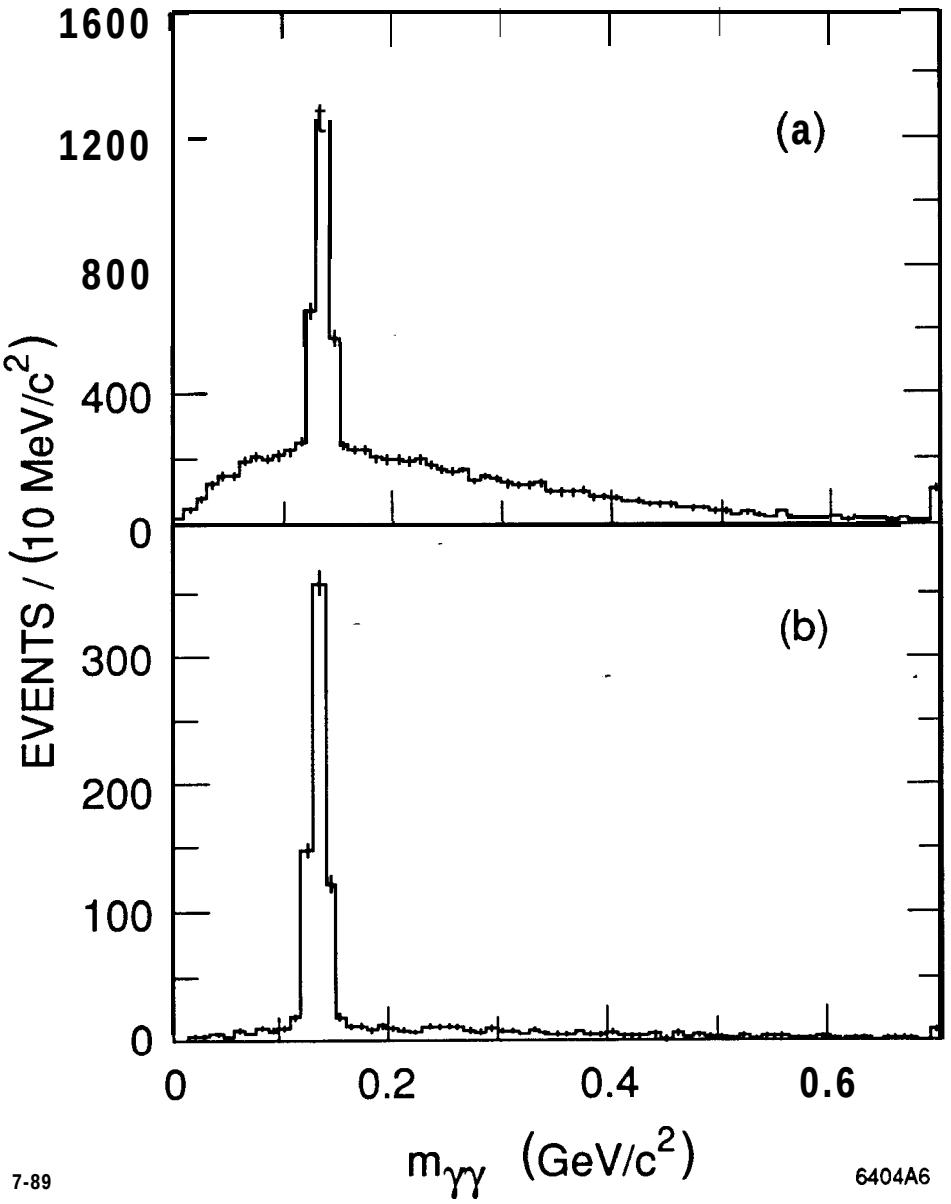
1600
1200
800
400
0
(a)
300
200
100
0
(b)
0
0.2
0.4
0.6
EVENTS / (10 MeV/c^2)
$m_{\gamma\gamma}$ (GeV/c^2)
7-89
6404A6

Fig. 6

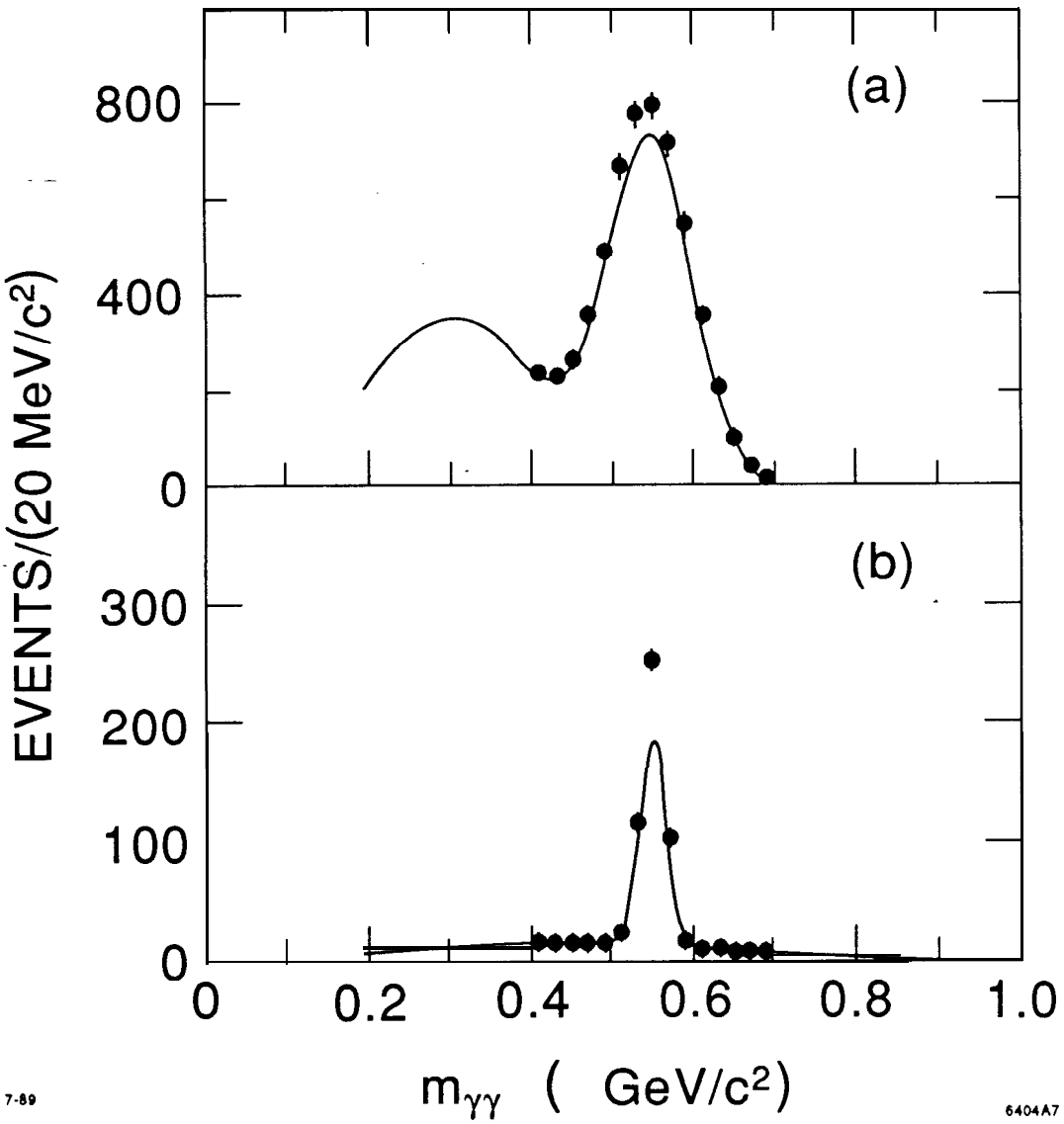
(a)
(b)
800
400
0
300
200
100
0
0
0.2
0.4
0.6
0.8
1.0
EVENTS/(20 MeV/c²)
mγγ (GeV/c²)
7-89
6404A7

Fig. 7

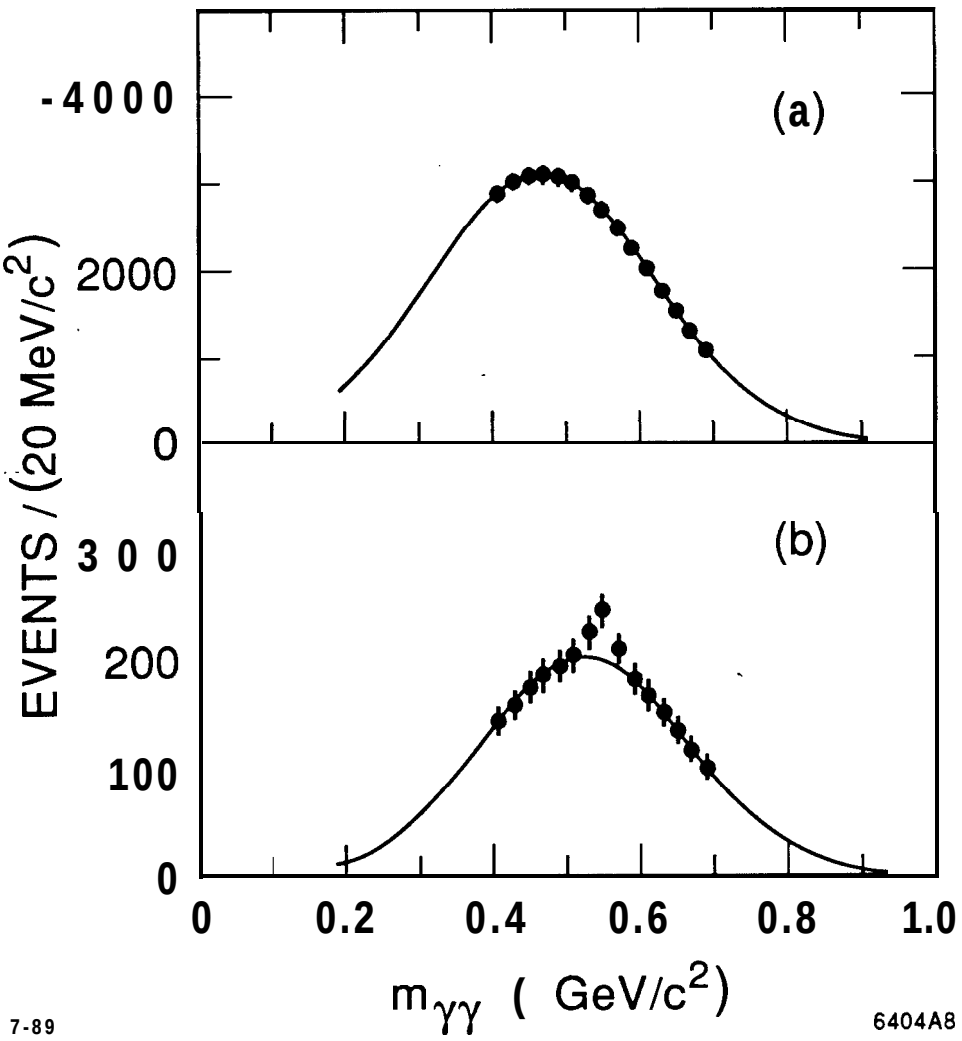
-4000
2000
0
(a)
EVENTS / (20 MeV/c^2)
300
200
100
0
(b)
0
0.2
0.4
0.6
0.8
1.0
$m_{\gamma\gamma}$ (GeV/c^2)
7-89
6404A8

Fig. 8

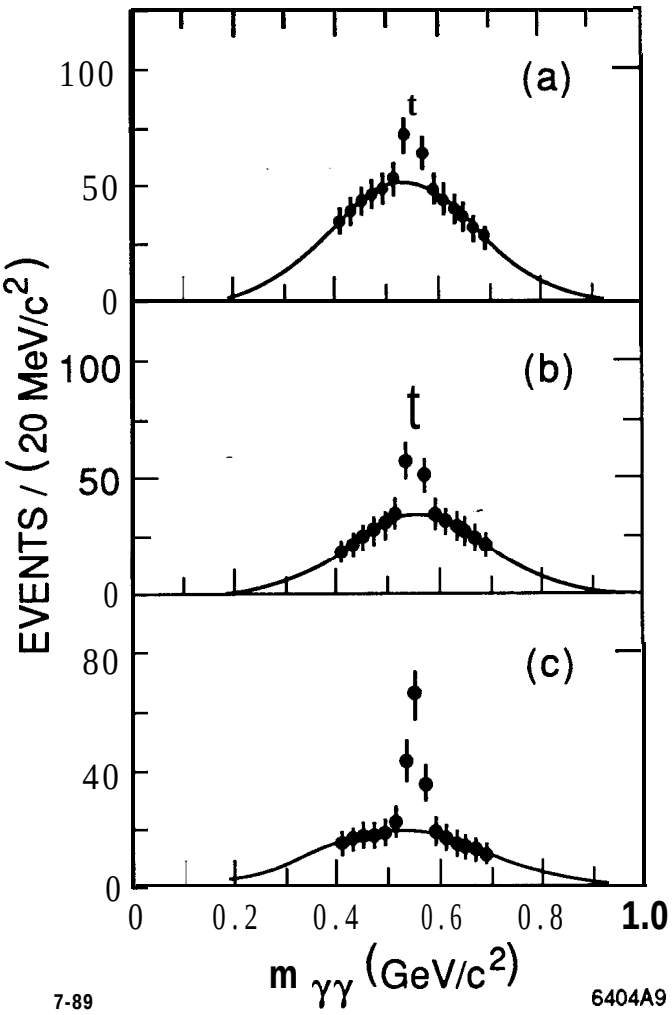
100
50
0
(a)
t
100
50
0
(b)
t
80
40
0
(c)
0
0.2
0.4
0.6
0.8
1.0
EVENTS / (20 MeV/c²)
m γγ (GeV/c²)
7-89
6404A9

Fig 9